SCIENCE CHINA
Information Sciences

• RESEARCH PAPER •
Special Focus on All Optical Networks

October 2016, Vol. 59 102305:1–102305:17
doi: 10.1007/s11432-016-0379-8

Lightpath blocking analysis for optical networks with ROADM intra-node add-drop contention

Yongcheng LI[1], Li GAO[1], Sanjay K. BOSE[2], Weidong SHAO[1],
Xiaoling WANG[1] & Gangxiang SHEN[1*]

[1]*School of Electronic and Information Engineering, Soochow University, Suzhou* 215006*, China;*
[2]*Department of Electronics and Electrical Engineering, Indian Institute of Technology, Guwahati* 781039*, India*

Received June 8, 2016; accepted July 13, 2016; published online September 12, 2016

Abstract The contention factor limits the extent to which lightpaths using the same wavelength can be added/dropped in a Reconfigurable Optical Add/Drop Multiplexer (ROADM) when it is operated in a colorless and directionless fashion. This paper presents an analysis to estimate the probability of blocked lightpath requests when a node of this type is used and validates the results for three traffic models. Simulations confirm the validity of the analytical results for lightpath blocking both for various values of the add/drop contention factor C and for changing load distribution in the network. We observe a saturation trend in the lightpath blocking performance as the add/drop port count per bank increases and that a high enough value of C reduces lightpath blocking to levels obtainable from an ideal, comntentionless ROADM. When C is small, limitations on the add/drop port count per bank is observed to be the dominant cause of blocking lightpaths while intra-node contention effects have only a limited impact. With increasing C, blocking is caused more because sufficient link capacity is not available and not because free add/drop ports are not available

Keywords contention factor, colorless, directionless, reconfigurable optical add/drop multiplexers (ROADMs), lightpath blocking

Citation Li Y C, Gao L, Bose S K, et al. Lightpath blocking analysis for optical networks with ROADM intra-node add-drop contention. Sci China Inf Sci, 2016, 59(10): 102305, doi: 10.1007/s11432-016-0379-8

1 Introduction

Reconfigurable optical add/drop multiplexers (ROADMs) can be remotely reconfigured, and would be a popular node technique for constructing a large-scale optical switched network [1, 2]. By enabling wavelengths to bypass intermediate nodes optically and therefore greatly reducing the need for regenerators, ROADMs provide significant cost savings. Different ROADM reconfiguration options have different impacts on lightpath blocking of optical transport networks. This paper evaluates these both through analysis and simulations.

* Corresponding author (email: shengx@suda.edu.cn)

1.1 Background

Dense wavelength division multiplexing (DWDM) is a promising technology for efficient data transmission in an optical transport network. Here, *lightpaths* carry traffic over an all-optical connection, where each lightpath corresponds to one wavelength channel crossing multiple fiber links along its route in the network. A lightpath starts at an optical transponder (ingress node), where the signal is *added*. While traversing the network towards its destination, the signal is optically switched at intermediate nodes. At a receiver, the signal is *dropped* by another transponder and converted back to the electrical format. As the core subsystem in the optical network, ROADMs realize the *add*, *drop*, and *bypass* functionalities needed by an all-optical lightpath [3–22].

Early OADMs had hard-wired optical components, where each change in node configuration required manual reconfiguration of the OADM. With the growth of applications where the traffic is highly dynamic, ROADMs which can be dynamically reconfigured with ease were introduced. In ROADMs, optical switching functionalities are realized by optical components that are driven by software, thereby supporting lightpath reconfigurations without manual intervention.

An important parameter for ROADMs is the number of switching degrees, i.e., the number of independent switching directions. Each degree is often associated with a pair of bi-directional fibers that connect the node to a neighbor node. Early ROADMs only supported two degrees and were employed in bi-directional rings [3]. The second generation of ROADMs enabled the capacity of multiple degrees for building complicated mesh networks. Having a greater number of degrees provides more flexibility as both the egress direction of an added lightpath and the ingress direction of a dropped lightpath can be changed.

The next generation of ROADMs in WDM networks would need to be *colorless*, *directionless*, and *contentionless*. These terms are briefly defined next. *Colorless* implies that any wavelength can be assigned to any of the add/drop ports of a ROADM. A ROADM is *directionless* if any wavelength from any nodal degree can be dropped at any drop port. A node suffers from *contention* (also sometimes referred to as *intra-node contention*) if the node has a common conflict point because of which more than one identical wavelengths are not allowed to go through the node. Contention may also happen if there is a common part which is being shared by multiple add/drop ports. This will lead to a contention if at least two identical wavelengths were to pass this common part [23, 24]. A ROADM will be *contentionless* if it does not have any such conflict point. It should be noted that realizing this contentionless feature would make the ROADM expensive. Therefore, in this paper, we focus on ROADMs which do have intra-node contention. Details on how intra-node contention can occur inside a ROADM node are further elaborated in Section 2.

1.2 Prior work

There have been studies to evalaute how the color, direction, and contention features of ROADMs have impacted lightpath blocking of an optical network. In this subsection, we review the related works on the evolution of the ROADM architecture and the analytical models for evaluating lightpath blocking performance.

An early mention in the literature of directionless and colorless ROADMs is found in [5–10]. More versatile ROADMs were subsequently presented in [11–20]. In [20], various flexible ROADM architectures and their implementations are proposed which are colorless, directionless, and contentionless with flexible channel bandwidth add/drop structures. Currently, because of high cost, ROADMs supporting the contentionless feature are not yet popular. However, most ROADMs available today do support the features of being colorless and directionless. In [21] and [22], the impact of intra-node contention was evaluated for an optical network under the static lightpath traffic demand assumption. It was found that a contention factor of $C = 2$ can achieve performance same as contentionless nodes. The key difference of the current research is that we aim to evaluate the impact of intra-node contention based on dynamic lightpath traffic demand, which is unpredictable and more challenging than the static lightpath traffic demand. There has been some research focusing on evaluating how intra-node contention affects node

lightpath blocking under dynamic lightpath demand [23–25]. In [23] and [24], intra-node blocking was considered for colorless and directionless ROADMs. Considering the situation where lightpath demands arrive randomly, the authors evaluated lightpath blocking and transponder usage for a single node using Monte Carlo simulations. The study in [25] investigated dynamic lightpath blocking for a network with colorless, non-directional ROADMs (CN-ROADMs).

It may be noted that, to date, only simulations have been reported for obtaining results for intra-node constraints when a ROADM is used in situations where the lightpath demand is dynamic. An alternative approach to analytically predicting lightpath blocking with the intra-node contention is a novel contribution of this paper. As mentioned in general in [26–43], this would be more desirable for the design and planning of networks as analytical methods not only give results faster and more conveniently than simulations, they would also allow a better understanding of the underlying behavior of the system. This has been attempted, for the first time in this paper, for ROADM nodes with intra-node contention.

Some early work based on analytical approaches for evaluation of lightpath blocking can be seen in [26–31] for single-fiber WDM networks. In [26], an approximate model for computing lightpath blocking was developed for static routing assuming the link load independence, both with and without wavelength conversion. This used a Poisson traffic model as this is the traditional model used for telephone traffic in typical telephone networks and has been commonly used by many researchers because of the analytical tractability of this model [28–31]. (We have also made this assumption in the subsequent work reported in this paper.) The approach proposed in [27] assumed that a wavelength is used on a link with a fixed probability that is independent from other wavelengths. Another model presented in [28] considered state-dependent arrival rates, and calculated lightpath blocking for two routing algorithms. Under dynamic traffic loading, approximate analytical models which formulated the cases with and without wavelength conversion capability have been considered in [29]. The simpler analytical model of [29] significantly reduces the computational complexity required. The study in [30] proposed an analytical model to calculate average lightpath blocking of an optical network with a limited wavelength conversion capability. It may be noted that the models employed in these papers assumed link load independence even though this would tend to overestimate the blocking probability (see the following paragraph). To take into account the correlation relationship between the wavelengths employed on the consecutive links traversed by a lightpath, the study in [31] developed a Markov chain model for DWDM networks with sparse wavelength conversion and without using wavelength converters. The model showed more accurate results for the blocking probability with only a moderate increase in the computational complexity.

Some researchers have also analyzed lightpath blocking under the scenario of multi-fibers per link. In [32], Li and Somani took link-load correlation into account in multi-fiber WDM networks. They not only compared the multi-fiber link load correlation model with the simulation results but also compared their results to the multi-fiber independent model presented in [33]. These results show that the multi-fiber independent model would underestimate the actual blocking probability. A simple analytical model for a multi-fiber network whose nodes have a limited range of wavelength conversion capability was also developed in [34].

All these models ignore the effects arising from the lack of free add/drop ports (i.e., transponders) at each node, which will impact the performance of a real system. The studies in [35] evaluated the performance of wavelength-routed optical networks both with and without wavelength conversion capability where the number of wavelengths per link and the number of add/drop ports per node are limited. Subramiam et al. [36] also examined the limitations from add/drop ports and their tunabilities. They also compared the performance between the cases of Share-Per-Link (SPL, the ports are dedicated to each link) and Share-Per-Node (SPN, all the links at a node share a pool of ports) in [36]. It was shown that the SPN case has a significant advantage over the SPL, when the numbers of add/drop ports are the same. A general analytical model for narrowly tunable transponders for the SPL case was developed in [37], and a similar analysis for the SPN case was presented in [38]. However, the color, direction and contention features were not taken into account.

Recently, we evaluated the performance of a colorless and directionless (CD) ROADM in comparison

with a colorless, directionless, and contentionless (CDC) ROADM in an optical transport network [39,40]. We developed analytical models and compared different methods for lightpath routing and selection of add/drop ports in terms of their lightpath blocking performance. We also found that the colorless capacity is important in reducing lightpath blocking. Furthermore, for a single ROADM node, we formulated an analytical model and studied how intra-node contention can impact lightpath blocking under different contention factors [42, 43]. The current study extends this from the single node case to an entire network.

1.3 Key contributions

We consider the impact on lightpath blocking of both intra-node contention and the add/drop contention factor C. A key contribution is to develop the analysis to estimate lightpath blocking approximately for an entire network that is made up of ROADMs with intra-node contention. A novel feature of our analytical approach is the introduction of an *auxiliary* link to model the intra-node contention of a ROADM node. Though our earlier analysis of [40] can model a network made up of CDC ROADMs, this paper, for the first time, presents an approach that can model a network made up of ROADMs with intra-node contention. Using this, we can now evaluate how lightpath blocking is affected by intra-node contention.

Additionally, we adopt different traffic load (distribution) models to test the accuracy of the analytical model. Our results indicate that the analytical model can predict lightpath blocking with reasonable accuracy. We observe that the different constraints play different roles in lightpath blocking under different values of C. When C is small, having only a limited number of add/drop ports dominates lightpath blocking while the intra-node contention effects have only a limited impact. With increasing C, blocking because of lack of free add/drop ports decreases, while blocking because of lack of link capacity and intra-node contention becomes more dominant. We also demonstrate the important conclusion that when C exceeds a threshold value, its impact on lightpath blocking is quite minimal. We observe similar saturation trends both between the add/drop port count per bank and lightpath blocking and between the contention factor C and lightpath blocking. By comparing with contentionless ROADM nodes, we find that a network made up of CD ROADMs with intra-node contention and a limited number of add/drop banks (i.e., contention factor C) can achieve a blocking performance of lightpaths similar to that of a network with CDC ROADMs, even though the latter would be considerably more expensive than the former. These results are a key conclusion of our work and would be important in designing practical networks at reasonable cost which would nevertheless provide superior performance.

Though the focus of our work on evaluating the impact of the contention factor C on lightpath blocking is similar to the works in [21] and [22], the following key differences may be observed. The studies in [21] and [22] were carried out based on a static lightpath traffic demand while our current study relies on dynamic lightpath traffic demand. This stochastic model would be practically more significant as demands in a real network would tend to be of this kind. The works in [21] and [22] were also mainly limited to using linear programming techniques and models for performance evaluation, while the current study develops a stochastic model to predict lightpath blocking for an optical network with intra-node contention ROADMs. Thus, though the two studies eventually reach similar conclusions on the impact of add/drop contention factor C, our approach is more general and has greater practical significance than that of [21] and [22].

1.4 Organization

We organize the rest of the paper as follows. The colorless and directionless ROADM architecture which does have intra-node contention is introduced in Section 2. Section 3 develops the analytical approach to evaluate lightpath blocking performance for this architecture. In Section 4, we present the performance evaluation conditions. The results of both the analytical models and simulations are presented in Section 5 and the paper concludes with Section 6.

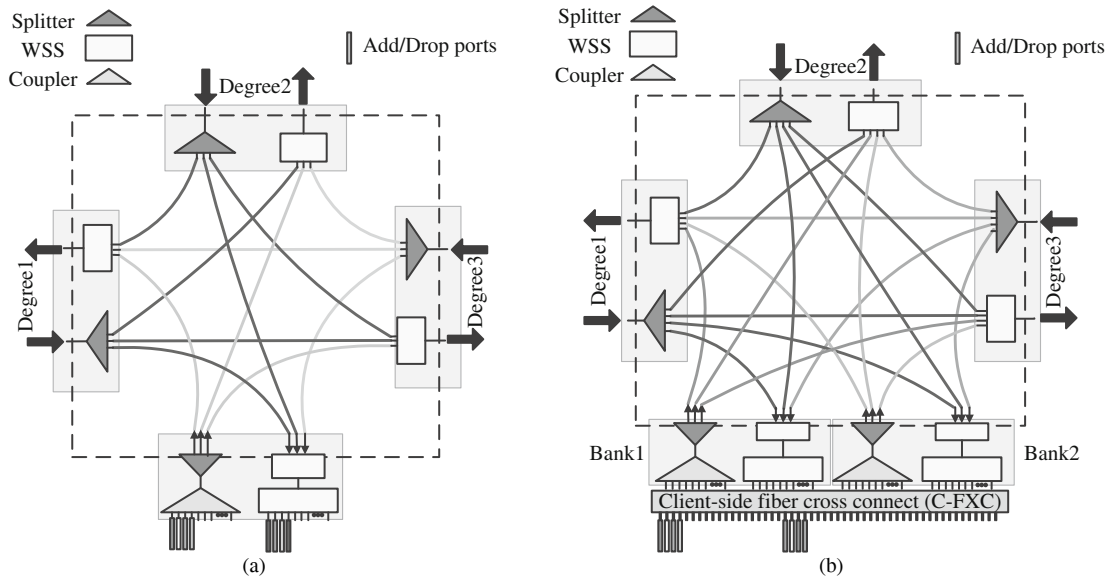

Figure 1 A ROADM architecture with intra-node contention. (a) Colorless, directionless ($C = 1$); (b) colorless, directionless ($C = 2$) [43].

2 Colorless and directionless ROADM architecture with intra-node contention

Today popular techniques for ROADMs are mostly based on the broadcast-and-select architecture, in which wavelength selective switches (WSSs) and optical splitters are often used. As an example, Figure 1 shows a ROADM architecture that contains three nodal degrees.

Figure 1(a) shows an example that supports both the colorless and directionless features. All the transponders can accept any wavelength and the signal of each transponder can be directed to any nodal degree. These transponders are accommodated in a common bank. For the add operation, the add module incorporates an optical coupler to combine the signals from all the transmitters followed by an optical splitter which subsequently distributes the signal in all possible directions. For the drop operation, a WSS first combines all the optical signals from different directions and transmits the combined signals to another WSS. This then separates the signals to the different drop ports. Note that in this type of architecture, contention exists on the common fiber segments between the splitter-coupler pair in the add direction and between the two WSSs in the drop direction. Here, it is impossible to add (or drop) two lightpaths of the same wavelength if they traverse the common parts, even if they are associated with different nodal degrees.

To resolve the contention constraint, we need an $N \times M$ WSS to replace the $1 \times M$ WSS. However, providing this kind of hardware is still challenging and expensive although some studies have been performed to address this [14–18] and some solutions have been proposed. Multiple $1 \times M$ WSS may also be used to alleviate the contention, but we would require C of them if it is designed to handle a *contention factor* of C [21]. Here, the *contention factor* C is defined as the maximum number of lightpaths with the same wavelength that can be added or dropped at a node. Figure 1(b) shows an example of this for the case of $C = 2$.

The node contention factor C equals the total number of add/drop port banks [21, 22]. The ROADM in Figure 1(a) has a single add/drop port bank, so $C = 1$. Similarly, the ROADM in Figure 1(b) has two add/drop port banks, so $C = 2$. Given a certain total number of add/drop ports, there would be less node intra-node contention and lower lightpath blocking if the contention factor C of the node is larger. For the case of Figure 1(b), it would be possible to share colorless add/drop ports between the various add/drop banks if a client-side fiber cross-connect (C-FXC) module is additionally incorporated.

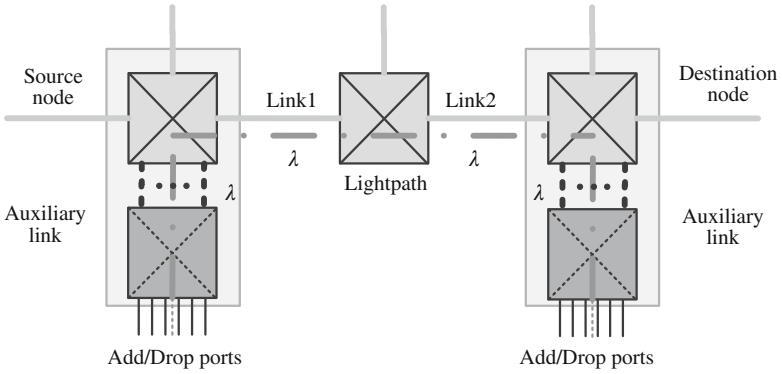

Figure 2 Lightpath and network models for performance analyses [43].

3 Analytical model

We present here a model to analyze how the intra-node contention can impact lightpath blocking as this would be of great significance in the overall performance of the system. It should be noted that the assumptions and some equations in the model have extended or reused those in the models developed for the WDM networks in the literature such as [26–43]. Our key contribution is to incorporate ROADM intra-node contention to model blocking of lightpaths. The ROADM architecture of Figure 1 (a) and (b) is considered for this study. We assume that the constraint of lightpath *wavelength continuity* [29] holds. As in [43], we assume the following for the traffic demand and lightpath routing strategies:

(1) As is usually done for analytical convenience, we assume a random Poisson model for the arrival requests of new lightpaths, where each granted request requires a random holding time with a negative exponential distribution, whose average is normalized to one unit (i.e., $1/\mu = 1.0$). These assumptions have been typically made to model random arrivals and service times, both in traditional circuit-switched networks and in WDM networks [28–31]. We follow a fixed shortest path routing strategy for establishing lightpaths between node pairs.

(2) As assumed in many analytical models [28–32], we also assume random wavelength assignment without any priority in the analytical model.

(3) It is assumed that the lightpath traffic loads on the links are independent of each other ignoring the potential correlation between traffic loads on the consecutive links of lightpaths when they are routed over a network. Even though this makes the model less accurate, it greatly simplifies its computational complexity. It should be noted that the detrimental effect of this assumption will be relatively more predominant in networks with low connectivity.

Next, we introduce the analytical model taking intra-node contention into account. To analyze how the availability of add/drop ports can affect lightpath establishment, we first see an example of a two-link lightpath as shown in Figure 2. As one of the important novel aspects of this study, the fiber that causes contention in each add/drop bank in Figure 1(b) is modelled as an *auxiliary* link. We also introduce two auxiliary nodes (i.e., the C-FXC module) at each of the two end nodes. If there are C add/drop banks, then there will be C such auxiliary links. Each auxiliary link carries the same number of wavelengths as a regular link.

As in [43], for a lightpath to be set up with a specific wavelength, the following three conditions must be satisfied:

(1) One free coloreless add/drop port must be available at each of the two lightpath end nodes.

(2) The wavelength thus used must also be available on at least one auxiliary link at each of the two lightpath end nodes.

(3) This wavelength must also be free on all the (regular) fiber links of the lightpath.

The notations used for the analysis are defined in the following, as in [43]:

T_i: the number of add/drop ports in each add/drop bank at node i.

C: the maximum number of lightpaths with the same wavelegnth to be added/dropped at the node,

which equals the number of auxiliary links or add/drop port banks. Thus, there will be a total of $T_i \cdot C$ add/drop ports at the node i.

W: the maximum number of wavelengths in both a regular fiber link and an auxiliary link.

$\lambda(s,d)$: for a pair of nodes (s, d), the lightpath traffic load offered between them.

$X_p(s,d)$: a count of the number of wavelengths which are free on the route between a pair of nodes (s, d) subject to the wavelength continuity constraint.

$\lambda_n(i)$: the total lightpath traffic load offered at node i.

$X_l(i)$: a count of the number of free wavelengths on (regular) link i.

$\alpha_i(\omega)$: the rate at which lightpaths are established (or set up) on link i given that there are ω free wavelengths available on the link.

$q_i(\omega) := P_r[X_l(i) = \omega]$ $(\omega = 1, \ldots, W)$ as the probability that ω wavelengths are free on link i.

$X_a(i)$: a count of the number of wavelengths which are free on auxiliary link i.

$f_l(i)$: the probability that on link i, a particular wavelength is free.

$\beta_i(\omega)$: the rate at which lightpaths are established (or set up) on auxiliary link i given that there are ω free wavelengths on the link.

$p_i(\omega) := P_r[X_a(i) = \omega]$ $(\omega = 1, \ldots, W)$ as the probability that ω wavelengths are free on auxiliary link i.

$f_a(i)$: the probability that on auxiliary link i, a particular wavelength is free.

$B_n(i)$: the probability that at node i, a lightpath is blocked due to the lack of free add/drop ports.

$P_b(s,d)$: the probability that between a pair of nodes (s, d), a lightpath is blocked.

P_B: the average probability that a lightpath is blocked in the entire network.

Using these notations, we compute the offered traffic load at node i in a network with CD add/drop ports as

$$\lambda_n(i) = \sum_j \lambda(i,j) \frac{1 - P_b(i,j)}{1 - B_n(i)}. \tag{1}$$

It may be noted that $\sum_j \lambda(i,j)(1 - P_b(i,j))$ computes the carried load of node i. This is a factor $1 - B_n(i)$ less than the total offered load at the node. Using the Erlang-B formula, the probability of blocking $B_n(i)$ at node i will then be

$$B_n(i) = E(\lambda_n(i), T_i) = \frac{\frac{\lambda_n(i)^{T_i \cdot C}}{(T_i \cdot C)!}}{\sum_{j=0}^{T_i \cdot C} \frac{\lambda_n(i)^j}{j!}}. \tag{2}$$

Using a birth-and-death as in [28–30] for modeling link wavelength status when there are ω free wavelengths on regular link i, we have

$$q_i(\omega) = \frac{W(W-1)\cdots(W-\omega+1)}{\alpha_i(1)\alpha_i(2)\ldots\alpha_i(\omega)} q_i(0), \quad \omega = 1, \ldots W, \tag{3}$$

where $q_i(0)$ is calculated as

$$q_i(0) = \left[1 + \sum_{\omega=1}^{W} \frac{W(W-1)\cdots(W-\omega+1)}{\alpha_i(1)\alpha_i(2)\ldots\alpha_i(\omega)}\right]^{-1}. \tag{4}$$

Given ω free wavelengths on the regular link i, the rate at which lightpaths are established (set up) on this link is obtained by summing the traffic contributed from all the lightpaths whose routes cross link i.

$$\alpha_i(\omega) = \begin{cases} 0, & \text{if } \omega = 0, \\ \sum\limits_{s,d;i\in\text{path}(s,d)} \lambda(s,d) P\{X_p(s,d) > 0 | X_l(i) = \omega\}, & \text{if } \omega = 1, \ldots, W. \end{cases} \tag{5}$$

Based on $q_i(\omega)$, we can further derive the probability $f_l(i)$ of a particular wavelength to be free on regular link i as

$$f_l(i) = q_i(1)\frac{1}{W} + q_i(2)\frac{2}{W} + \cdots + q_i(W) = \sum_{k=1}^{W} q_i(k)\frac{k}{W}. \tag{6}$$

The term $q_i(k)\frac{k}{W}$ calculates the probability that a certain wavelength λ is available on link i given that there are k wavelengths available on this link where we assume an equal load on each wavelength.

We can develop essentially similar equations for auxiliary link i. Using our earlier equations for calculating $q_i(\omega)$ for the regular link i, the same equations for $p_i(\omega)$ for auxiliary link i are obtained by replacing $\alpha_i(\omega)$ with $\beta_i(\omega)$.

$$p_i(\omega) = \frac{W(W-1)\cdots(W-\omega+1)}{\beta_i(1)\beta_i(2)\cdots\beta_i(\omega)} p_i(0), \quad \omega = 1,\ldots W, \tag{7}$$

where

$$p_i(0) = \left[1 + \sum_{\omega=1}^{W} \frac{W(W-1)\cdots(W-\omega+1)}{\beta_i(1)\beta_i(2)\cdots\beta_i(\omega)}\right]^{-1}. \tag{8}$$

Similarly, the lightapth establishing (or setup) rate $\beta_i(\omega)$ on auxiliary link i when there are ω wavelengths free on it is

$$\beta_i(\omega) = \begin{cases} 0, & \text{if } \omega = 0, \\ \sum\limits_{s,d;i=s \text{ or } i=d} (\lambda(s,d)/C) P\{X_p(s,d) > 0 | X_a(i) = \omega\}, & \text{if } \omega = 1,\ldots,W. \end{cases} \tag{9}$$

Here the term $\sum_{s,d;i=s \text{ or } i=d}(\lambda(s,d)/C)$ calculates the average offered traffic load on each add/drop bank in the source or destination node. $\sum_{s,d;i=s \text{ or } i=d}\lambda(s,d)$ is the total offered load from all the lightpath routes, of which node i is the source or destination node. Because there are C add/drop banks in the node, we need to divide by C to get the average traffic load on each bank.

Based on $f_l(i)$, we derive the probability $f_a(i)$ that a particular wavelength is free on auxiliary link i, similarly by replacing $q_i(\omega)$ with $p_i(\omega)$.

$$f_a(i) = p_i(1)\frac{1}{W} + p_i(2)\frac{2}{W} + \cdots + p_i(W) = \sum_{k=1}^{W} p_i(k)\frac{k}{W}. \tag{10}$$

For a lightpath to be successfully established between two end nodes, we need to ensure that a common wavelength must be free on all the regular links traversed along the route of the lightpath, at least one free auxiliary link at each of the two end nodes of the lightpath and at least one free add/drop port is available at both the end nodes of the lightpath. With this, the probability of successfully establishing a lightpath given ω wavelengths free on regular link i is derived as

$$\begin{aligned} P_r[X_p(s,d) > 0 | X_l(i) = \omega] &= (1 - B_n(s))(1 - B_n(d)) \times \\ &\left(1 - \prod_{j=1}^{\omega}\left(1 - \left(1 - (1 - f_a(s))^C\right) \times \left(1 - (1 - f_a(d))^C\right) \prod_{k\in\text{path}(s,d);k\neq i} f_l(k)\right)\right). \end{aligned} \tag{11}$$

Here $(1-(1-f_a(i))^C)$ is the probability that a wavelength is available on the auxiliary links of node i (i.e., the end nodes of the lightpath), the term $(1-B_n(s))(1-B_n(d))$ computes the probability that both end nodes of the lightpath have free add/drop ports, and the term $\prod_{k\in\text{path}(s,d);k\neq i} f_l(k)$ is the probability that a particular wavelength is free on all the regular links (excluding link i) traversed by the lightpath.

Similarly, given that ω wavelengths are free on auxiliary link i, the probability that a lightpath is successfully established is

$$\begin{aligned} &P_r[X_p(s,d) > 0 | X_a(i) = \omega] \\ &\quad = (1 - B_n(s))(1 - B_n(d))\left(1 - \prod_{j=1}^{\omega}\left(1 - \left(1 - (1 - f_a(r))^C\right) \prod_{k\in\text{path}(s,d)} f_l(k)\right)\right), \end{aligned} \tag{12}$$

where if $i = s$, then $r = d$; otherwise, $r = s$.

The overall probability that a lightpath is blocked between a pair of nodes $(s,\ d)$ can be formulated as

$$P_b(s,d) = 1 - (1 - B_n(s))(1 - B_n(d)) \ \times \left(1 - \prod_{j=1}^{\omega}\left(1 - \left(1 - (1 - f_a(s))^C\right) \times \left(1 - (1 - f_a(d))^C\right) \prod_{k\in \mathrm{path}(s,d)} f_l(k)\right)\right). \quad (13)$$

In (13), $(1 - B_n(s))(1 - B_n(d))$ ensures at least one free add/drop port each at the two end nodes of the lightpath. $(1 - (1 - f_a(s))^C)$ says that there is a specific free wavelength in the *auxiliary* link in the source node and $(1 - (1 - f_a(d))^C)$ says that there is a specific free wavelength in the *auxiliary* link in the destination node. $\prod_{k\in \mathrm{path}(s,d)} f_l(k)$ means that there is a specific wavelength commonly free on the all the fiber links along route between a pair of nodes s and d.

$\prod_{j=1}^{\omega}(1 - (1 - (1 - f_a(s))^C) \times (1 - (1 - f_a(d))^C) \ \prod_{k\in \mathrm{path}(s,d)} f_l(k))$ means that all the ω wavelengths are not available between the node pair.

Thus, $1 - \prod_{j=1}^{\omega}(1 - (1 - (1 - f_a(s))^C) \times (1 - (1 - f_a(d))^C) \ \prod_{k\in \mathrm{path}(s,d)} f_l(k))$means that there is at least one wavelength available between the node pair.

$(1 - B_n(s))(1 - B_n(d)) \times (1 - \prod_{j=1}^{\omega}(1 - (1 - (1 - f_a(s))^C) \times (1 - (1 - f_a(d))^C) \ \prod_{k\in \mathrm{path}(s,d)} f_l(k)))$ is the probability of successfully establishing a lightpath between the node pair.

The overall lightpath blocking probability of the entire network can then be finally computed and is given by

$$P_B = \frac{\sum_{s,d} P_b\,(s,d)\,\lambda\,(s,d)}{\sum_{s,d} \lambda\,(s,d)}. \quad (14)$$

An iterative relaxation method is to calculate average probability of lightpath blocking over the entire network. In the iterative process, let $\lambda_n^k(i), B_n^k(i), f_a^k(i), \beta_i^k(\omega), f_l^k(i), \alpha_i^k(\omega), p_i^k(\omega), q_i^k(\omega), P_b^k(s,d)$, and P_B^k be the values obtained from $\lambda_n\,(i)\,, B_n\,(i)\,, f_a\,(i)\,, \beta_i\,(\omega)\,, f_l\,(i)\,, \alpha_i\,(\omega)\,, p_i\,(\omega)\,, q_i\,(\omega)\,, P_b\,(s,d)$ and P_B in the kth iteration. We give the detailed steps for this next.

(1) Let $B_n^0\,(i)$, $P_b^0\,(s,d)$, and P_B^0 be 0 and choose $f_a^0\,(i)$ and $f_l^0\,(i)$ to be any arbitrary value between 0 and 1.0.

(2) Set $k = 1$.

(3) Use (1) to calculate $\lambda_n^k\,(i)$ and (2) to get $B_n^k\,(i)$.

(4) Use (5) and (11) to calculate $\alpha_i^k\,(\omega)$ and find $\beta_i^k\,(\omega)$ using (9) and (12).

(5) Use (3) and (4) to calculate $q_i^k\,(\omega)$ and use (7) and (8) to get $p_i^k\,(\omega)$.

(6) Use (6) to calculate $f_l^k\,(i)$ and use (10) to calculate $f_a^k\,(i)$.

(7) Use (13) to calculate $P_b^k(s,d)$).

(8) Use (14) to find P_B^k. If $|\ P_B^k - \ P_B^{k-1}| < \varepsilon$, then terminate; otherwise, set $k = k + 1$ and repeat from Step 3.

It should be pointed out that this iterative relaxation process, though easy to implement, sometimes (but very rarely) has a problem in converging to the solution. When that happens, a simple fix is to repeat the iteration process with a slightly different set of initial conditions until convergence is obtained. Other more advanced numerical methods that ensure the convergence (such as the Newton method as suggested in [44]) may also be used if convergence is indeed observed to be a problem in the above computations.

Also, the current analytical model takes the assumption of link independence of traffic load. The results shown in Section 5 will validate the effectiveness of this simplified assumption. A model considering the link traffic correlation (including between regular and auxiliary links) may be proposed as in [31, 32]. Though that would be more accurate, considerably more computational effort would then be needed than in the method proposed by us here.

4 Performance evaluation conditions

We assume a dynamic lightpath traffic model in our simulation studies where random lightpath requests arrive following a Poisson arrival process and have holding times which are random with a negative

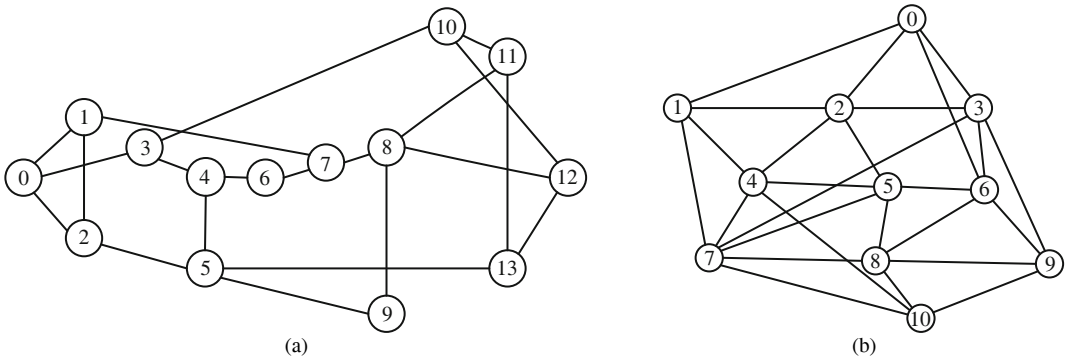

Figure 3 Test networks. (a) 14-node, 21-link NSFNET network; (b) 11-node, 26-link COST239 network.

exponential distribution (with unity mean), as given earlier. All the regular links are identical and have the same number of wavelengths in the networks. All the auxiliary links are also considered to be identical. The NSFNET network (14 nodes, 21 links) and the COST239 network (11 nodes, 26 links) were used for our test studies. These networks are shown in Figure 3. For each lightpath blocking performance test, we simulated a total of 10^6 lightpath arrival requests. To ensure that the results obtained from the simulations are valid, we vary the traffic load until the blocking probability is no smaller than 10^{-5}.

To evalaute the accuracy of the analytical model, we have also considered three different traffic load distribution patterns in addition to the model of same traffic load per node pair. These three traffic load models are as follows:

4.1 Average distributed traffic load model

In this model, the traffic load (in units of Erlangs) between each node pair is assumed to fluctuate randomly within a range whose average is fixed. For this, apart from assuming an *average traffic load* of l Erlangs, we also assume a *range* Δ Erlang such that the traffic load varies randomly within the interval of $(l - \Delta, l + \Delta)$ Erlang.

4.2 Distance based traffic load model

For different lightpaths, the number of route hops may be different with a longer lightpath contributing more to the overall effective network load. Under this traffic load model, the traffic load between a pair of nodes is assumed to be inversely proportional to the hop count of the shortest route between each node pair. With this assumption, the traffic load of a longer lightpath is proportionally lower than that of a shorter lightpath so that their contributions to the overall effective network traffic load are the same. For this model, we define the *basic traffic load* contributed to the network by a lightpath as *the product of the traffic load of the node pair of the lightpath and the number of hops of the lightpath.* A lightpath with h hops carrying an end-to-end traffic load of λ/h Erlang will contribute a basic effective traffic load λ Erlang to the overall network (i.e., sum of the traffic load over each of its h hops); or equivalently, a lightpath with basic traffic load λ Erlang and h hops has an end-to-end traffic of λ/h Erlang.

4.3 Hub node based traffic load model

In a network, some nodes can have higher nodal degrees while others can have lower nodal degrees. These higher degree nodes may act as hub nodes in the network. These nodes would tend to carry higher traffic loads, so the traffic loads from the hub nodes or to the hub nodes are assumed to be greater than that between the regular (non-hub) nodes. We define a "hub node pair" as one where at least one of the nodes is a hub node and a "regular node pair" as one where both the nodes are non-hub nodes. When we use this model, we select 20% of the nodes as hub nodes according to their nodal degrees going from the highest to the lowest.

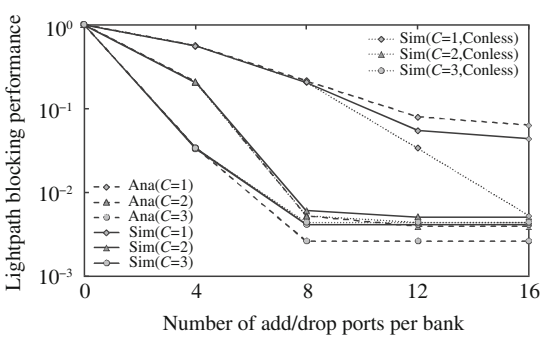

Figure 4 Lightpath blocking performance versus limited numbers of add/drop ports per bank in the NSFNET network (offered traffic load: 0.5 Erlang per node pair; Ana: Analysis; Sim: Simulation; Conless: Contentionless).

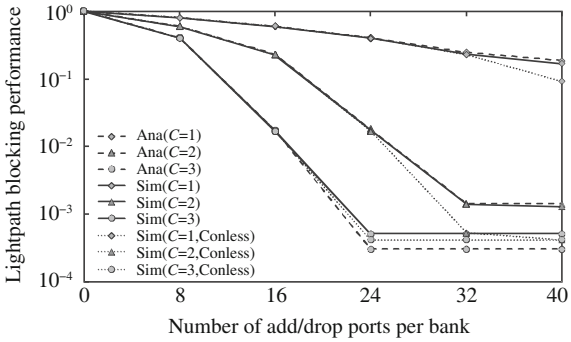

Figure 5 Lightpath blocking performance versus limited numbers of add/drop ports per bank in the COST239 network (offered traffic load: 3.6 Erlang per node pair; Ana: Analysis; Sim: Simulation; Conless: Contentionless).

5 Result analyses

5.1 Uniform traffic load

Here, we assume the same offered traffic load per node pair. We adopt different numbers of wavelengths for different networks for better performance comparison. The NSFNET network is assumed to have 16 wavelengths in each link and the COST239 network is assumed to have 40 wavelengths in each link. The random wavelength assignment strategy and the fixed shortest path routing algorithm are applied in the simulations to match the assumptions in the analytical model.

In this subsection, we show the results for various example optical networks. Figures 4 and 5 show the lightpath blocking probabilities subject to T add/drop ports per add/drop bank at each node. Here, we assume T to be identical for all the nodes. The lightpath blocking performances are estimated both through the analytical model and the simulations given 0.5-Erlang offered traffic load per node pair in NSFNET and 3.6-Erlang offered traffic load per node pair in COST239[1)]. It is observed that the analytical results and the simulation results match well. We also observe that given a certain number of add/drop banks, C, the blocking probability for the lightpaths reduces as the number of add/drop ports per bank, T increases. We also observe a saturation effect here, i.e., when T reaches a certain level, its further increase does not improve lightpath blocking significantly. For example, in the NSFNET network, we see that when the add/drop port count per bank exceeds 12, the lightpath blocking probability for contention factor $C = 1$ is nearly saturated. For $C = 2$ and 3, the saturation points occur earlier, when there are eight add/drop ports per bank. Similar saturation effects are observed for the COST239 network. This saturation phenomenon was also pointed out in [21] and [22], even though the results there were based on a static lightpath traffic demand. This saturation trend shows an important design consideration since it indicates that once this saturation condition is reached, adding more add/drop ports would increase the system cost without sufficient performance improvement to justify this cost increase.

Figures 4 and 5 also exhibit similar performance saturation on the number of add/drop banks C. In Figure 4, for the NSFNET example, when C increases from 1 to 2, a notable decrease is observed in the lightpath blocking probability; however, when C increases further from 2 to 3, the reduction in lightpath blocking probability is much smaller than before. This is reasonable since a larger C means more add/drop ports at each node. Since the average degree of NSFNET is between 2 and 3, when C is equal to 2 or 3, each node already has sufficient add/drop ports for each wavelength incident to the node (i.e., each wavelength can almost always be assigned with a dedicated add/drop port) leading to the saturation effect as observed. Similar observations can be made and explained for the COST239 network as shown in Figure 5.

1) We choose the Erlang load value between each node pair in the two test networks subject to the condition that the lightpath blocking probabilities are within the range from 10^{-5} to 10^{-1} when the blocking probabilities become saturated with an increasing add/drop port count per bank.

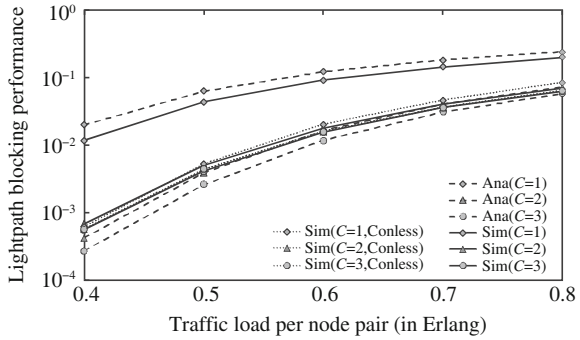

Figure 6 Lightpath blocking performance versus traffic load (in Erlang) per node pair in the NSFNET network (16 add/drop ports per bank; Ana: Analysis; Sim: Simulation; Conless: Contentionless).

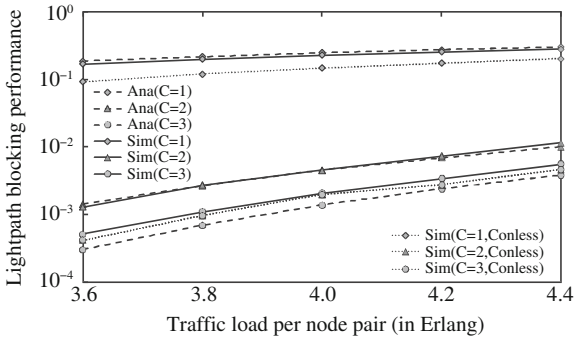

Figure 7 Lightpath blocking performance versus traffic load (in Erlang) per node pair in the COST239 network (40 add/drop ports per bank; Ana: Analysis; Sim: Simulation; Conless: Contentionless).

For the blocking performance shown in both Figures 4 and 5, we find that when the contention factor is $C = 1$, the analytical results are slightly higher than those obtained through simulations. However, when the contention factors are $C = 2$ or 3, this effect is reversed. This is also reasonable because when $C = 1$, the analytical model ignores the neighboring (regular) link-load correlation of a lightpath, leading to an over-estimated blocking probability as also reported in [31]. In contrast, when $C = 2$ or 3, each source and destination node has multiple (auxiliary) links which have a parallel link-load correlation. Since we ignored this for simplicity, the actual blocking probability is under-estimated as reported in [32].

Finally, we also compare the results of the networks made up of ROADMs with and without intra-node contention. We see that for a small contention factor C (i.e., $C = 1$), the contentionless case starts to show a lower lightpath blocking probability when the add/drop port count per bank is larger than 8 for NSFNET and greater than 32 for COST239. However, for larger contention factors C (i.e., $C = 2$ and 3), we observe a small performance difference of lightpath blocking between the cases with and without intra-node contention. This means that increasing C from 1 to 2 can significantly alleviate lightpath blocking due to the intra-node contention. This implies that it is not necessary for a ROADM to incorporate the expensive contentionless feature so as to achieve good lightpath blocking performance if we can guarantee sufficient add/drop ports in each bank.

Figures 6 and 7 show the lightpath blocking performance trend from a different perspective, i.e., with increasing offered load per node pair by fixing the number of add/drop ports per bank (i.e., 16 for NSFNET and 40 for COST239). We again observe that the analytical results closely match the results obtained through simulations. A saturation trend is once again observed with increase in the number of add/drop port banks C. In addition, when the contention factor C is small, the contentionless case shows much better lightpath blocking performance. However, when C is larger ($C = 2$ and 3), the difference between the blocking performances of the cases with and without intra-node contention is minor. We also find that we can increase the contention factor C to achieve better performance with lower cost, e.g., by using $C = 2$ in the NSFNET and COST239 networks.

It may be noted that to successfully provision a lightpath, the following three conditions must be met: (1) sufficient link capacity should be available, (2) no intra-node contention at the two end nodes of the lightpath, and (3) free add/drop ports available at the two end nodes of the lightpath. Lightpath blocking will occur if any of these conditions are not met. It would, therefore, be important to study how each of these contributes to overall lightpath blocking. We present the percentage of each blocking type obtained by simulations for the NSFNET and COST239 networks in Figure 8. To generate these results, we check first for link blocking, then for contention blocking, and lastly for port blocking where multiple conditions may occur for the blocking observed. Figure 8(a) shows these blocking percentage results for the NSFNET network that has 8 add/drop ports per bank in each node. Figure 8(b) shows the blocking percentage results for the COST239 network that has 24 add/drop ports per bank in each node. Legend "LB" means blocking because of insufficient link capacity, "CB" means blocking because of intra-node

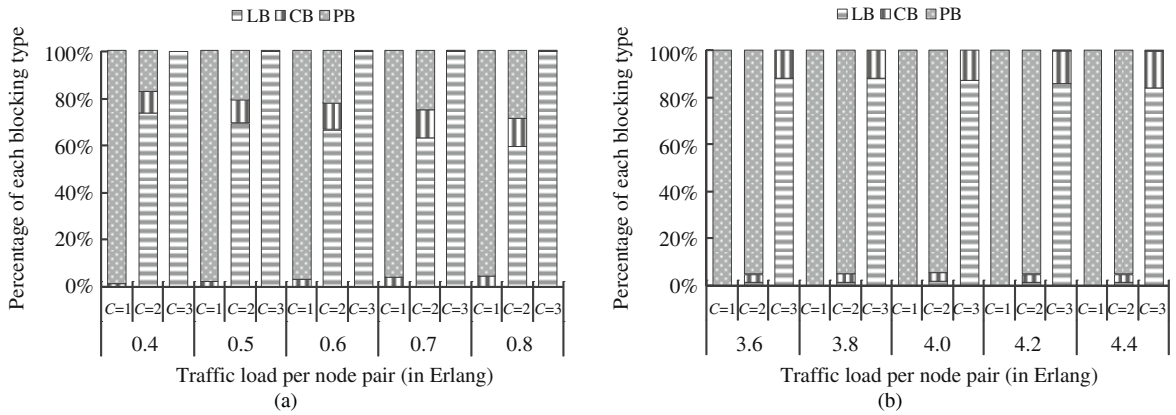

Figure 8 Lightpath blocking percentage distribution due to different types of blocking constraints: link capacity blocking, intra-node contention blocking, and add/drop port blocking (NSFNET: 8 add/drop ports per bank; COST239: 24 add/drop ports per bank). (a) NSFNET; (b) COST239.

contention, and "P" corresponds to blocking because of no free add/drop ports.

For the NSFNET network, we see that under a small contention factor C (i.e., $C = 1$), the constraint of free add/drop ports plays a dominant role in blocking. A small contribution is from the constraint of intra-node contention but blocking because of insufficient link capacity is absent. However, with an increasing contention factor C (i.e., $C = 2$), which means more add/drop ports, the contribution to blocking because of lack of add/drop ports becomes less in overall blocking; blocking due to the link capacity constraint increases and so does contention blocking. If we further increase C to 3, there are sufficient add/drop ports. Blocking because of no free add/drop ports disappears while blocking due to the link capacity constraint becomes dominant.

Similar blocking behavior is observed for the COST239 network. The only difference with the NSFNET network is that the intra-node contention factor seems to play a more important role with an increasing add/drop factor C. When $C = 3$, contention blocking is still significant, though link capacity blocking is dominant. The reason for this is that the average nodal degree of the COST239 network is higher than that of the NSFNET. The COST239 network, therefore, requires a larger contention factor C to fully eliminate blocking due to intra-node contention.

5.2 Other traffic load models

The blocking performance results for the three modified traffic load models described in Section 4 have also been obtained and are shown here. As before, we assume 16 wavelengths per fiber link for the NSFNET network and 40 wavelengths per fiber link for the COST239 network. We show simulation results for both fixed shortest path routing and random wavelength assignment.

Figures 9–16 show lightpath blocking under the different traffic models for the NSFNET and COST239 networks. Specifically, Figures 9 and 10 show the results for the *average distributed traffic load model*, Figures 11 and 12 show the results of the *distance based traffic load model* and Figures 13–16 present the results of the *hub node based traffic load model*. For both of the networks, the performance is very similar to those obtained using the uniform traffic load. The analytical results can well predict the results obtained by the simulations with intra-node contention taken into account. Also, under these traffic load distributions, we see that the results of the networks made up of ROADMs with and without intra-node contention are close to each other when C reaches a certain level. (Due to space constraints, we have not shown the results for the contentionless case.)

Under the average distributed traffic load model, the analytical model can adapt to the random variations in the traffic load incorporated in the model. Figure 9 shows the results for the NSFNET network. Here, Figure 9 keeps the average traffic load at 0.5 Erlang with a variation range of 0.2 Erlang and demonstrates the performance with changing numbers of add/drop ports per bank. The corresponding

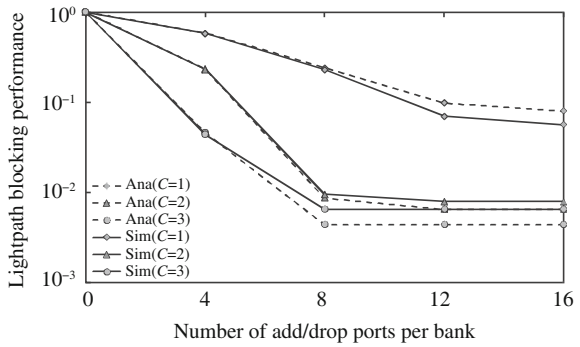

Figure 9 Lightpath blocking performance versus limited numbers of add/drop ports per bank in the NSFNET network under average distributed traffic load model (traffic model 1; average offered load: 0.5 Erlang per node pair; variation range: 0.2 Erlang; Ana: Analysis; Sim: Simulation).

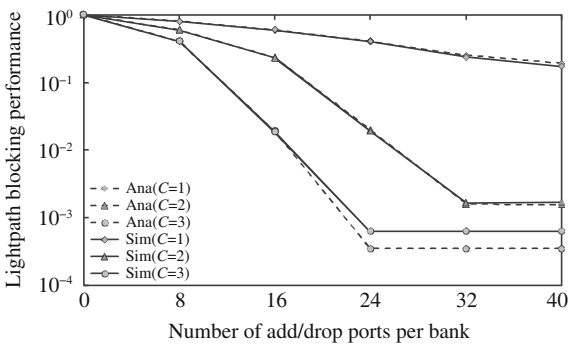

Figure 10 Lightpath blocking performance versus limited numbers of add/drop ports per bank in the COST239 network under average distributed traffic load model (traffic model 1; average offered load: 3.6 Erlang per node pair; variation range: 0.2 Erlang; Ana: Analysis; Sim: Simulation).

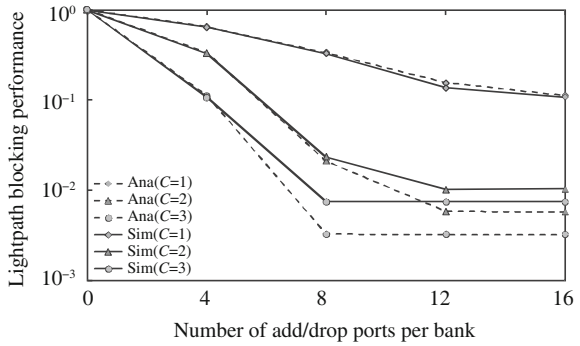

Figure 11 Lightpath blocking performance versus limited numbers of add/drop ports per bank in the NSFNET network under distance based traffic load model (traffic model 2; basic offered load: 1.2 Erlang per node pair; Ana: Analysis; Sim: Simulation).

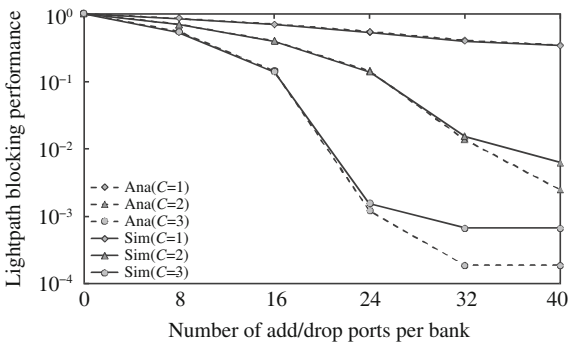

Figure 12 Lightpath blocking performance versus limited numbers of add/drop ports per bank in the COST239 network under distance based traffic load model (traffic model 2; basic offered load: 6.6 Erlang per node pair; Ana: Analysis; Sim: Simulation).

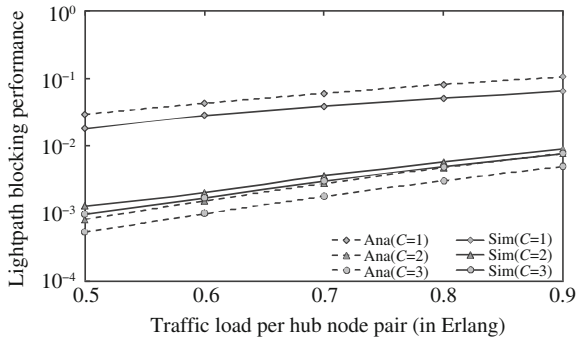

Figure 13 Lightpath blocking performance versus traffic load (in Erlang) per node pair in the NSFNET network under hub node based traffic load model (traffic model 3; 16 add/drop ports per bank; offered load per regular node pair: 0.4 Erlang; Ana: Analysis; Sim: Simulation).

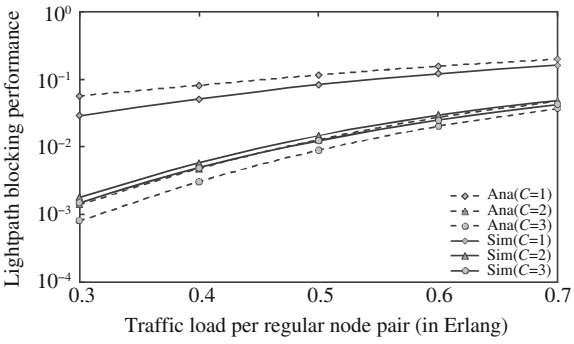

Figure 14 Lightpath blocking performance versus traffic load (in Erlang) per node pair in the NSFNET network under hub node based traffic load model (traffic model 3; 16 add/drop ports per bank; offered load per hub node pair: 0.8 Erlang; Ana: Analysis; Sim: Simulation).

performance results are shown in Figure 10 for the COST239 network. We observe that, in all cases, the analytical results are very close to those obtained through the simulations. This validates our proposed analytical approach.

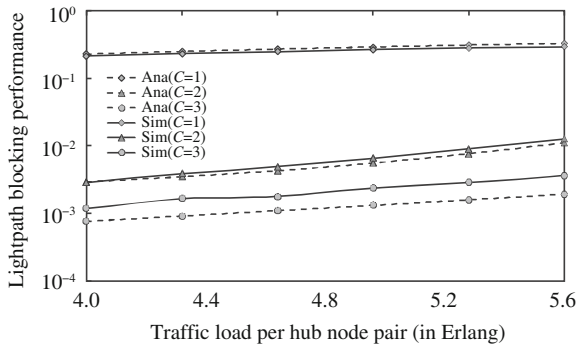

Figure 15 Lightpath blocking performance versus traffic load (in Erlang) per node pair in the COST239 network under hub node based traffic load model (traffic model 3; 40 add/drop ports per bank; offered load per regular node pair: 3.8 Erlang; Ana: Analysis; Sim: Simulation).

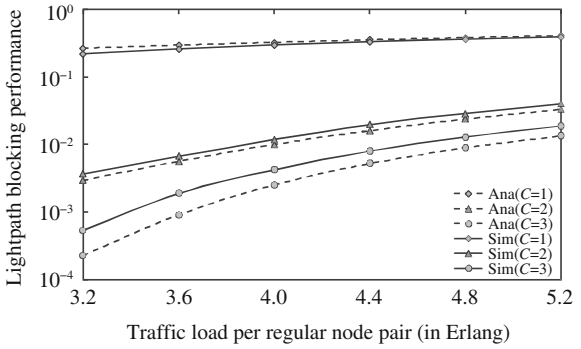

Figure 16 Lightpath blocking performance versus traffic load (in Erlang) per node pair in the COST239 network under hub node based traffic load model (traffic model 3, 40 add/drop ports per bank; offered load per hub node pair: 5.6 Erlang; Ana: Analysis; Sim: Simulation).

The results for the distance based traffic load model are shown in Figures 11 and 12 for the NSFNET and COST239 networks, respectively. Here, the *basic traffic load* (as defined in Subsection 4.2) per node pair is 1.2 Erlang in Figure 11 for the NSFNET network and 6.6 Erlang in Figure 12 for the COST239 network. As in the earlier case, we find that for both networks, the analytical results are very close to those obtained through the simulations.

Finally, Figures 13–16 show the results obtained by applying the hub node based traffic load model to both the networks. We keep the add/drop port count per bank at 16 for NSFNET network and 40 for COST239 network and change the average traffic load per node pair. Figures 13 and 15 fix the traffic load of a regular node pair and vary the traffic load per hub node pair. Similarly, Figures 14 and 16 change the traffic load per regular node pair by fixing the traffic load per hub node pair. Based on these results, we can again see that the results from the analytical model matches well those obtained through simulations.

6 Conclusion

This paper presents results on the impact of ROADM intra-node contention on the blocking performance of lightpaths using both a new analytical model and through simulations. A novel feature of the modeling approach is that of modeling the intra-node contention of the ROADM node by introducing an *auxiliary* link. To confirm the analytical model accuracy, three different traffic load distribution patterns have been considered. The results indicate that the analytical model accurately predicts the blocking performance of lightpaths under various combinations of add/drop contention factor C, the add/drop port count per bank T, and the offered traffic load per node pair. When C is small, having a limited number of add/drop ports becomes the dominant factor for lightpath blocking while intra-node contention shows only a limited impact. With increasing C, blocking because of no free add/drop ports is reduced significantly, while blocking because of insufficient link capacity becomes dominant, and the intra-node contention factor becomes strong. We also note that there is only a minor impact on lightpath blocking when C exceeds a certain level. We also observe two saturation trends between the add/drop port count per bank and the number of add/drop banks versus the lightpath blocking performance. When the add/drop port count per bank reaches a certain level, further increase in the number of add/drop ports per bank leads to only slight performance improvement. We also observe a saturation effect in the lightpath blocking performance with a growing number of add/drop banks. Our results show that increasing the contention factor C can dramatically reduce the lightpath blocking probability. However, it is meaningful to note that when this add/drop contention factor C reaches a certain level, the performance achieved by a cheaper ROADM subject to intra-node contention is almost as good as a much more expensive contentionless ROADM.

Acknowledgements This work was jointly supported by National Natural Science Foundation of China (Grant Nos. 61322109, 61671313, 61172057), Natural Science Foundation of Jiangsu Province (Grant Nos. BK20130003, BK2012179), and Science and Technology Support Plan of Jiangsu Province (Grant No. BE2014855).

Conflict of interest The authors declare that they have no conflict of interest.

References

1 Berthold J, Saleh A A M, Blair L, et al. Optical networking: past, present, and future. J Lightw Technol, 2008, 26: 1104–1118
2 Keyworth B P. ROADM subsystems and technologies. In: Proceedings of Optical Fiber Communication Conference, Anaheim, 2005. 1–4
3 Earnshaw M P, Soole J B D. Integrated reconfigurable optical wavelength add-drop multiplexer. Electron Lett, 2002, 38: 1351–1352
4 Ennser K, Rogowski T, Ghelfi P, et al. Reconfigurable add/drop multiplexer design to implement flexibility in optical networks. In: Proceedings of 2006 International Conference on Transparent Optical Networks, Nottingham, 2006. 74–77
5 Chen J, Jacob J, Santivanez C, et al. En route to grouping-constraint free, colorless directionless ROADMs. In: Proceedings of National Fiber Optic Engineers Conference, San Diego, 2010. 1–3
6 Roorda P, Collings B. Evolution to colorless and directionless ROADM architectures. In: Proceedings of National Fiber Optic Engineers Conference, San Diego, 2008. 1–3
7 Collings B. Physical layer components, architectures and trends for agile photonic layer mesh networking. In: Proceedings of European Conference on Optical Communication, Vienna, 2009. 1–3
8 Thiagarajan S, Blair L, Berthold J. Direction-independent add/drop access for multi-degree ROADMs. In: Proceedings of Optical Fiber Communication Conference, San Diego, 2008. 1–3
9 Kim I, Palacharla P, Wang X, et al. Performance of colorless, non-directional ROADMs with modular client-side fiber cross-connects. In: Proceedings of National Fiber Optic Engineers Conference, Los Angeles, 2012. 1–3
10 Thiagarajan S, Asselin S. Nodal contention in colorless, directionless ROADMs using traffic growth models. In: Proceedings of National Fiber Optic Engineers Conference, Los Angeles, 2012. 1–3
11 Zami T. Contention simulation within dynamic, colorless and unidirectional/multidirectional optical cross-connects. In: Proceedings of European Conference and Exposition on Optical Communications, Geneva, 2011. 1–3
12 Abedifar V, Shahkooh S A, Emami A, et al. Design and simulation of a ROADM-based DWDM network. In: Proceedings of Iranian Conference on Electrical Engineering, Mashhad, 2013. 1–4
13 Ji P N, Aono Y. Colorless and directionless multi-degree reconfigurable optical add/drop multiplexers. In: Proceedings of Annual Wireless and Optical Communications Conference, Shanghai, 2010. 1–5
14 Jensen R, Lord A, Parsons N. Colorless, directionless, contentionless ROADM architecture using low-loss optical matrix switches. In: Proceedings of European Conference and Exhibition on Optical Communication, Torino, 2010. 1–3
15 Jensen R, Lord A, Parsons N. Highly scalable OXC-based contentionless ROADM architecture with reduced network implementation costs. In: Proceedings of Optical Fiber Communication Conference, Los Angeles, 2012. 1–3
16 Jensen R. Optical switch architectures for emerging colorless/directionless/contentionless ROADM networks. In: Proceedings of Optical Fiber Communication Conference, Los Angeles, 2011. 1–3
17 Devarajan A, Sandesha K, Gowrishankar R, et al. Colorless, directionless and contentionless multi-degree ROADM architecture for mesh optical networks. In: Proceedings of International Conference on Communication Systems and Networks, Bangalore, 2010. 1–10
18 Way W, Ji P N, Patel A N. Contention resolution within colorless and directionless ROADM. In: Proceedings of National Fiber Optic Engineers Conference, Anaheim, 2013. 1–3
19 Džanko M, Mikac B, Miletić V, et al. Analytical and simulation availability models of ROADM architectures. In: Proceedings of International Conference on Telecommunications, Zagreb, 2013. 39–46
20 Gringeri S, Basch B, Shukla V, et al. Flexible architectures for optical transport nodes and networks. IEEE Commun Mag, 2010, 48: 40–50
21 Pavon-Marino P, Bueno-Delgado M V. Dimensioning the add/drop contention factor of directionless ROADMs. J Lightw Technol, 2011, 29: 3265–3274
22 Pavon-Marino P, Bueno-Delgado M V. Add/drop contention-aware RWA with directionless ROADMs: the offline lightpath restoration case. IEEE J Opt Commun Netw, 2012, 4: 671–680
23 Woodward S L, Feuer M D, Palacharla P, et al. Intra-node contention in a dynamic, colorless, non-directional ROADM. In: Proceedings of Optical Fiber Communication Conference, San Diego, 2010. 1–3
24 Feuer M D, Woodward S L, Palacharla P, et al. Intra-node contention in dynamic photonic networks. J Lightw Technol, 2011, 29: 529–535
25 Palacharla P, Wang X, Kim I, et al. Blocking performance in dynamic optical networks based on colorless, non-directional ROADMs. In: Proceedings of National Fiber Optic Engineers Conference, Los Angele, 2011. 1–3
26 Kovacevic M, Acampora A. On wavelength translation in all-optical networks. In: Proceedings of Annual Joint Conference of the IEEE Computer and Communications Societies, Bringing Information to People, Boston, 1995. 413–422
27 Barry R A, Humblet P A. Models of blocking probability in all-optical networks with and without wavelength changers.

IEEE J Sel Areas Commun, 1996, 14: 858–867
28 Birman A. Computing approximate blocking probabilities for a class of all-optical networks. IEEE J Sel Areas Commun, 1996, 14: 852–857
29 Shen G X, Bose S K, Cheng T H, et al. Performance analysis under dynamic loading of wavelength continuous and non-continuous WDM networks with shortest-path routing. Int J Commun Syst, 2001, 14: 407–418
30 Tripathi T, Sivarajan K N. Computing approximate blocking probabilities in wavelength routed all-optical networks with limited-range wavelength conversion. In: Proceedings of Annual Joint Conference of the IEEE Computer and Communications Societies, New York, 1999. 329–336
31 Subramaniam S, Azizoglu M, Somani A K. All-optical networks with sparse wavelength conversion. IEEE ACM Trans Netw, 1996, 4: 544–557
32 Li L, Somani A K. A new analytical model for multifiber WDM networks. IEEE J Sel Areas Commun, 2000, 18: 2138–2145
33 Subramaniam S, Barry R A. Wavelength assignment in fixed routing WDM networks. In: Proceedings of International Conference on Communications, Montreal, 1997. 406–410
34 Shen G X, Cheng T H, Bose S K, et al. Approximate analysis of limited-range wavelength conversion all-optical WDM networks. Comput Commun, 2001, 24: 949–957
35 Shen G X, Bose S K, Cheng T H, et al. The impact of the number of add/drop ports in wavelength routing all-optical networks. Opt Netw Mag, 2003, 4: 112–122
36 Turkcu O, Subramaniam S. Blocking and waveband assignment in WDM networks with limited reconfigurability. In: Proceedings of Optical Fiber Communication Conference, Anaheim, 2007. 1–3
37 Turkcu O, Subramaniam S. Blocking in reconfigurable optical networks. In: Proceedings of International Conference on Computer Communications, Anchorage, 2007. 188–196
38 Turkcu O, Subramaniam S. Blocking analysis of limited reconfigurable optical networks. In: Proceedings of International Conference on Computer Communications and Networks, Honolulu, 2007. 216–221
39 Li Y C, Gao L, Peng L M, et al. Modeling the impact of ROADM color and directional constraints on optical network performance. In: Proceedings of Asia Communications and Photonics Conference, Guangzhou, 2012. 1–3
40 Li Y C, Gao L, Shen G X, et al. Impact of ROADM colorless, directionless, and contentionless (CDC) features on optical network performance. J Opt Commun Netw, 2012. 4: B58–B67
41 Gao L, Li Y C, Shen G X. Lightpath blocking performance analytical model for ROADMs with intra-node add/drop contention. In: Proceedings of International Conference on Communications in China, Shanghai, 2014. 97–101
42 Gao L, Liu H, Li Y C, et al. Modeling impact of ROADM intra-node add/drop contention on a single node lightpath blocking performance. China Commun, 2015, 12: 89–98
43 Gao L, Li Y C, Shen G X. Modeling the impact of ROADM intra-node add/drop contention on optical network performance. In: Proceedings of Asia Communications and Photonics Conference, Beijing, 2013. 1–3
44 Girard A. Routing and Dimensioning in Circuit Switched Networks. Boston: Addison-Wesley Longman Publishing Co., Inc., 1990